Alexandria Engineering Journal (2021) 60, 1465–1476

HOSTED BY

ELSEVIER

Alexandria University

Alexandria Engineering Journal

www.elsevier.com/locate/aej
www.sciencedirect.com

Second law efficiency analysis of air injection into inner tube of double tube heat exchanger

Nazaruddin Sinaga [a,*], **Saleh khorasani** [b,*], **Kottakkaran Sooppy Nisar** [c], **Amr Kaood** [d]

[a] *Mechanical Engineering Department, Engineering Faculty of Diponegoro University, Indonesia*
[b] *Department of Mechanical Engineering, Urmia University, Urmia, Iran*
[c] *Department of Mathematics, College of Arts and Sciences, Prince Sattam bin Abdulaziz University, Wadi Aldawaser 11991, Saudi Arabia*
[d] *Mechanical Engineering Department, Faculty of Engineering, Fayoum University, El-Fayoum 63514, Egypt*

Received 16 August 2020; revised 15 October 2020; accepted 30 October 2020
Available online 7 December 2020

KEYWORDS

Double-tube heat exchanger;
Two-phase flow;
Effectiveness-NTU;
Overall heat transfer coeffOverall heat transfer coefficient;
Dimensionless exergy loss;
Witte-Shamssundar efficiency (η_{w-s})

Abstract At present study, thermal performance of a double tube heat exchanger due to stream of air/water two phase flow through inner tube is experimentally studied. Air and hot water were mixed in a T-junction outside heat exchanger and then were followed into inner tube of heat exchanger. Told water flow rate was kept constant and was equal to 2 lit/min. For hot water flow rate, four different flow rates of 3, 4, 5 and 6 lit/min was considered. Also inlet temperature of cold and hot water streams were almost constant and were within range of 17–19 °C and 48–50 °C. Also, for air flow rate five different flow rates of 1, 2, 3, 4 and 5 lit/min were considered. Volume fraction was within the range of 0.14 and 0.62. Obtained results were analyzed based on several energetic and exergitic parameters including pressure drop, effectiveness, Number of Transfer Units, heat transfer coefficient, dimensionless exergy loss and Witte-Shamsundar efficiency factor. Results presented an increment of 33% and 38% in heat transfer coefficient and Number of Transfer Units, respectively. Maximum value of Witte-Shamsundar efficiency factor was found to be 0.973 and was related to Volume fraction of 0.57 and has occurred at counter flow.

1. Introduction

Through the last decades, the fast progress in industrial activities has led to emission of lots of greenhouse gases [1] which has provided many problems to the human life and has made them to try to reduce the production of this gases as best as possible [2]. Researchers have proposed different methods for solving this problem as like to using renewable energy sources [3] efficiency improvement methods [4] and etc. Amongst efficiency improvement activities, improving the performance of

* Corresponding authors at: Jalan Prof. Soedarto, SH Tembalang, Semarng, Central Java, Indonesia (N. Sinaga).
E-mail addresses: nsinaga19.undip@gmail.com (N. Sinaga), Khorasani.saleh@yahoo.com (S. khorasani), n.sooppy@psau.edu.sa, ksnisar1@gmail.com (K. Sooppy Nisar), amrkaood@fayoum.edu.eg (A. Kaood).

Peer review under responsibility of Faculty of Engineering, Alexandria University.

https://doi.org/10.1016/j.aej.2020.10.064

Nomenclature

Q_{air}	Air flow rate (lit/min)
Q_w	Water flow rate (lit/min)
U	Overall heat transfer coefficient (W/m^2K)
$\dot{m}$	Mass flow rate (Kg/s)
d_h	Hydraulic diameter (m)
T	Temperature (K)
ΔT	Temperature difference (K)
Q	Heat transfer (J/s)
ΔT_{LMTD}	Logarithmic mean temperature difference (K)
E	Exergy destruction (W)
s	Entropy (J/K)
S_{gen}	Entropy generation (J/K)
T_e	Environmental temperature (K)
e	Dimensionless exergy loss
W_R^+	Uncertainty of dependent variables
W_i	Uncertainty of independent variables
X_i	Independent variables
ΔP	Pressure drop (Pa)
NTU	Number of transfer units
ε	Effectiveness
C_p	Specific heat (J/kg·K)
L	Length of tube (m)
VF	Volume fraction

Subscripts

e	Environment
i	inlet
o	outlet
i	inner
tp	Two-phase
sp	Single-phase
c	cold
h	hot
min	Minimum

thermal systems has gained significant attractions, because this system either use the energy, transfer it or exchange the form of energy. Anyway, improvement of the efficiency of thermal systems has environmental, economic and operational advantages and has great importance for the thermal engineers [5]. Amongst various thermal equipment, the heat exchangers are very attractive for engineers [6]. This equipment plays critical role in industries including thermal applications. Consequently, any method that could help to improve the energy efficiency of this instruments would lead to efficiency improvement of the whole system and will bring economic and environmental advantages. During recent decades, engineers and experts have proposed a wide range of methods to improve the thermal performance of heat exchangers. These methods are mainly divided into two main categories namely as active and passive methods. The passive methods are those type of mechanisms at which no external forces are used and generally include the use of different type of inserts [7,8], corrugated walls [9], fins [10] and addition of nano-particles to the working fluid [11]. On the other side, the active methods are those in which the external force is the agent of the heat transfer enhancement factor [12]. Amongst various active heat transfer methods, the air injection or more generally, the use of gas–liquid two-phase flow has gained significant attention [13]. Due to the turbulent nature of the mentioned flow, the heat transfer coefficient in such flows has more values when compared single-phase flows [14,15]. Besides, the turbulent nature of the two-phase flow prevents the sedimentation of the solid particles of the flow and reduces the negative effects of the fouling phenomena . All these together have made the use of two-phase flow as an effective method in the heat exchangers. At the following a brief summary of both active and passive methods applied for the performance improvement of heat exchangers is provided.

Khwayyir et al. [16] performed experiments to investigate the effect of air injection on the performance of double tube heat exchanger which was integrated with solar panel. Baqir et al. [17] conducted experiments to investigate the influence of air injection on the thermal performance of helical coil tube heat exchanger. Their results presented up to 1.93 times increment in the Number thermal units (NTU). Qi et al. [18] carried out experimental research to find the effect of nano-fluids on heat transfer and pressure drop of double-tube heat exchanger. Through their study the influence of various affecting parameters including water flow rates, nano-fluid concentration, nano-fluids locations, Re number of nano-fluids and inner tube structure were examined. Also, in another study, Qi et al. [19] investigated the thermal and flow characteristics of nano-fluids for different corrugation pitches. Moreover, in another study, they used nano-fluids and twisted-tape turbulator inside a triangle tube to analyze their effect based on energy and exergy concepts [19]. Nakhchi and Esfahani [20] performed a numerical simulation to check the effect of inserting double V-cut twisted tapes on the thermal performance of double tube heat exchanger. Through their study, different geometrical characteristics of twisted-tape was considered. Karimi et al. [21] using a two-phase mixture model, simulated the simultaneous effect of using twisted tape and nano-fluids in a double-tube heat exchanger. Also, they considered the effect of surface roughness (material type) to evaluate the effect of roughness on the pressure drop and thermal performance at the presence of nano-fluid and turbulator. Yadav and Sahu [22] evaluated the performance enhancement of double-tube heat exchanger through experimental tests. The outer wall of the inner tube was equipped with helical surface disc turbulators. Hot water flowed through the inner tube while cold air passed from annular space. Different operating parameters including diameter ratios, helix angle and Reynolds number were considered in their study to find out the optimum operating conditions. Heyhat et al. [23] conducted an experimental study and investigated the thermal behavior of a DTHE due to injecting air into the outer tube of DTHE. Through their study, the effect of different injection mechanisms was considered. Also, the angle of double tube heat exchanger was considered as an investigating factor. Deng et al. [24] investigated the performance of a finned double tube heat exchanger utilized in a latent heat thermal storage system. Bashtani et al. [25] numerically investigated the effect of wall corrugation on the

performance of double tube heat exchanger. Gnanavel et al. [26] reported up to %70 augmentation at the performance of double tube heat exchanger due to the simultaneous usage of nano particles and circular fin inserts. Dizaji and Jafarmadar [27] studied the effect of air injection into the double tube heat exchanger. In this study, they placed a plastic tube inside the inner tube of the heat exchanger. The plastic tube had some tiny holes by which the air was injected into the heat exchanger. Khorasani and Dadvand [28] experimentally investigated the influence of air bubble injection into the shell side of a shell and coiled tube heat exchanger on the thermal performance. For this purpose, a plastic tube circulated along the inner side of bottom wall of the shell and covered the lower half section of the shell. The duty of this tube, in which there were small holes, was to disperse the bubble evenly to increase the turbulence intensity and increase the heat transfer between shell and coiled tube. In this regard, Moosavi et al, [29] injected air bubbles from the bottom of the vertical shell and coiled tube heat exchanger. They announced that this mechanism helps the improvement of heat transfer since bubbles upward departure increases turbulence intensity of the flow. Subsequently, this phenomenon causes an increment in the overall heat transfer coefficient of the shell and coiled tube heat exchanger.

The present study, has the following worthy points. **First-The injection method:** almost all the studies existed in the literature have used the injection methods that are fabricated within the double tube heat exchangers [25,29]. However, this method could not be used for the heat exchangers that are currently in use, because they need to be either redesigned or reinstalled. Both of redesigning and reinstallation need financial investments. However, the method presented in this paper, could be added to the present systems thus it is a separated system and could be easily fabricated in all heat exchangers. **Second: Efficiency analysis from the perspectives of bot first law and second law of thermodynamics:** As is known, double tube heat exchangers are one of those very important part of thermal systems as like to power plants, refinery systems and etc. Since analysis based on first law and second law of thermodynamics play a key role on the efficiency evaluations, it is very important to have a clear view of each part of the whole system. Furthermore in this study the White Shamsunder efficiency (η_{w-s}) which covers concepts based on both on first law and second law of thermodynamic and was presented for this type of heat exchangers (it should be noted that parameters like effective ness and dimensionless exergy destruction are based on one of laws of thermodynamics). Consequently, due to the fact that heat exchangers are one of the most important parts of thermal systems, evaluation of this instruments from different perspectives (with any new thermal performance enhancement method) would be very valuable for engineers and experts.

2. Experimental study

2.1. Experimental setup

The schematic and general illustration of the experimental apparatus are shown in Fig. 1(A) and (B). According to this layout, the setup is a compound of four main parts as follows:

(i) The cooling unit: This part consists of a cold water reservoir, control valves, water pump, and water Rota-meter.
(ii) The heating unit: including hot water reservoir, water pumps, control valves, water Rota-meter, and secondary hot water reservoir.
(iii) Air supply unit: composed of air compressor, control valves, air Rota-meter, and mixing section.
(iv) The testing unit: compound of a double-tube heat exchanger, data logger, and manometer.

To supply the required air flow, a conventional air compressor (refrigerator compressor) was used. The volumetric flow rate of the air stream was measured by means of an air Rota-meter (model KHL-08A01M-V) right before the inlet of mixing chamber. A 12-Channel Lutron (BTM4208SD) data-logger with K-type thermocouples were exerted to measure and record the temperatures of intended sections (Points 1, 2, 3 and 4 on the Fig. 1(A), which are associated to inlet and outlet temperatures of hot and cold water streams). In order to check the accuracy and reliability of data-logger, an ice-water bath was used for calibrating. For measuring the pressure drop through the inner outer tube a Lutron manometer (PM-9100) was used. The probes of digital manometer were fabricated on the presented points on Fig. 1(A) (Points 1, 2, 3 and 4). The geometrical specifications of the double-tube heat exchanger are provided in Table 1. The inner tube and outer tube was made of copper and steel, respectively. The outer surface of the outer tube was properly insulated with glass wool to minimize the heat exchange with ambient which was surveyed by energy balance. A gauged cylinder was employed to calibration of flow-meters. With this aim, the filling time of a certain volume of a cylinder was recorded by a chronometer and then was compared with the measured value of flow-meter. The geometrical specifications of the double-tube heat exchanger are provided in Table 1.

2.2. Experimental procedure

Table 2 presents the procedure of considered tests. The hot water was warmed up to 49 ± 1 °C and then was pumped to the mixing section. As presented in Fig. 1, two control valves (using bypass method) were used for controlling the volumetric flow rate of the hot water. The hot water was measured with a Rota-meter which was calibrated at the temperature of hot stream. The hot water flow rate varied between 3 lit/min to 6 lit/min (3, 4, 5, 6 lit/min). At the air supply unit, the air (with temperature of 20 °C) was injected into the mixing chamber where it was mixed with hot water stream. The mixing chamber was exactly like which Khorasani et al. [9] had used. Also, there was a distance of 70 cm between the mixing section and the entrance of the heat exchanger for better mixing and accuracy of results. The airflow rate was adjusted by two control valves as shown in Fig. 1 (A). For each hot water flow rate, the volumetric flow rate of air was changed from 0 lit/min to 5 lit/min. Hot water and airflow met each other at the mixing chamber and then the resultant two-phase flow entered the inner tube of the double-tube heat exchanger. Furthermore, at the cooling unit, tap water flow (with temperature of 17 + 0.5 °C) filled the cold water tank and then was pumped to the outer tube of the heat exchanger. The cold water flow was kept constant at 2 lit/min. The cold water flow rate was adjusted via control valves which were fabricated on the main path line and by pass line. Also, for

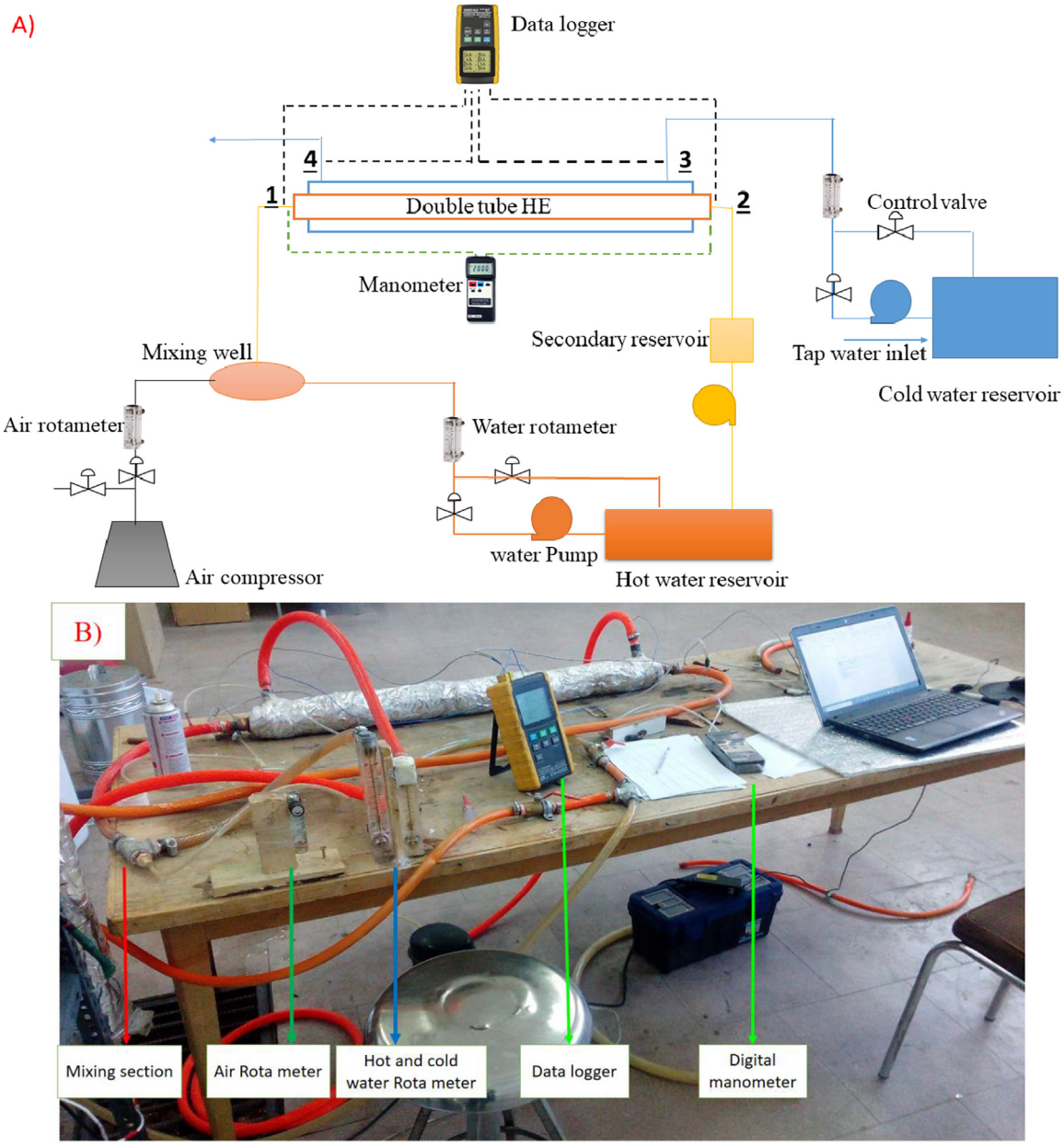

Fig. 1 Schematic view (A) and General view and (B) of the present setup.

Table 1 Geometrical specifications of tubes.

Tube	Inner Diameter (mm)	Length (mm)	Thickness (mm)
Inner tube	26	1000	2.1
Outer tube	44.1	1000	3

measuring the value of volumetric flow rate of cold water stream a Rota-meter was used. On every inlet and outlet of the heat exchanger, the thermocouples of data-logger and probes of manometer (pressure drop measurement probes) were fabricated to sense the temperature and pressure drop values, respectively. The hot water stream after exiting the heat exchanger was directed to the secondary reservoir to re-obtain its lost heat and reach again to the temperature of 49 °C. Then the hot water with the required temperature was pumped to the main tank. It is worth mentioning that at the present study, the heat transfer between hot water and air was neglected. This was due to a very less mass flow rate and latent heat capacity of air in comparison with hot water [9–11] and [28]. Also, as mentioned before, there was a distance of 70 cm between the mixing section and the entrance of the two phase flow into the inner tube, where the inlet temperature of the hot water flow was measured. Through this distance the two streams found thermally equilibrium condition which minimized the effect of temperature difference between two phases on the thermal results. Indeed, a very important advantage of the aforementioned method for providing two-phase flow was the more accurate thermal results. However, the direct

Table 2 General information on tested conditions (variable parameters are bold in each row).

	Flow specifications					Thermodynamic specifications		Geometrical specifications	
	$\dot{Q}_{W,inner}$(lit/min)	$\dot{Q}_{A,inner}$(lit/min)	VF	$\dot{Q}_{W,outer}$(lit/min)	Flow direction	$T_{C,inlet}$(°c)	$T_{h,inlet}$(°c)	D_{inner}(Inner tube), mm	D_{inner}(outer tube), mm
Effect of inner tube water-phase flow rate	**3, 4, 5, 6**	0	0	2	Counter & Parallel	17–19	48–50	26	44.1
	3, 4, 5, 6	1	0.25, 0.2, 0.16, 0.14	2	Counter & Parallel	17–19	48–50	26	44.1
	3, 4, 5, 6	2	0.4, 0.3, 0.28, 0.25	2	Counter & Parallel	17–19	48–50	26	44.1
	3, 4, 5, 6	3	0.5, 0.42, 0.37, 0.33	2	Counter & Parallel	17–19	48–50	26	44.1
	3, 4, 5, 6	4	0.57, 0.5, 0.44, 0.4	2	Counter & Parallel	17–19	48–50	26	44.1
	3,4, 5, 6	5	0.62, 0.55, 0.5, 0.45	2	Counter & Parallel	17–19	48–50	26	44.1
Effect of inner tube air-phase flow rate	3	**0, 1, 2, 3, 4, 5**	0, 0.25, 0.4, 0.5, 0.57, 0.62	2	Counter & Parallel	17–19	48–50	26	44.1
	4	**0, 1, 2, 3, 4, 5**	0, 0.2, 0.3, 0.42, 0.5, 0.55	2	Counter & Parallel	17–19	48–50	26	44.1
	5	**0, 1, 2, 3, 4, 5**	0, 0.16, 0.28, 0.37, 0.44, 0.5	2	Counter & Parallel	17–19	48–50	26	44.1
	6	**0, 1, 2, 3, 4, 5**	0, 0.14, 0.25, 0.33, 0.4, 0.45	2	Counter & Parallel	17–19	48–50	26	44.1

injection methods which were presented in the literature [25,30] and [29], didn't allowed the two phases to get thermally equilibrium, so that there was the possibility of sensing the temperature of air slugs, and as a result, there was more potential of inaccuracy.

2.3. Experimental uncertainty

Regardless of skill of operator and accuracy of measurement devices, all experimental measurements involve uncertainty. This is because of both imperfection of measuring instruments, precision of recording data and operator skill. In fact, uncertainty can be defined as the difference in the gauged value and actual value of a certain parameter. Through present study, the proposed method of Moffat [30] is used for calculating the uncertainty values. This method has been extensively used by numerous authors [30,31,34] and [33] and is defined following:

$$W_R^+ = \left[\left(\frac{\partial R^+}{\partial X_1}W_1\right)^2 + \left(\frac{\partial R^+}{\partial X_2}W_2\right)^2 + \cdots + \left(\frac{\partial R^+}{\partial X_n}W_n\right)^2\right]^{1/2} \quad (1)$$

where X_i (i = 0, 1, 2, …, n) presents the independent variables, also W_i (i = 0, 1, 2, …, n) is the uncertainty of independent variables. The obtained results for the uncertainty of both dependent and independent parameters are provided in the table 3. It is worth mentioning that the obtained results for the uncertainty values are in the range uncertainty values of papers which was previously published in this filed [30,31].

3. Parameter definition and calculations

3.1. Calculation of dimensionless exergy destruction

Exergy is defined as the potential of available energy when converting it to useful work. Indeed, it is the amount of work that can be extracted from certain energy. Exergy is a type of energy and its unit is exactly like the unit of energy (kJ, kJ/kg, and kW are exergy units). Actually, Exergy is part of the energy which can be converted into work. In the exergy calculation, we assume that all processes are ideal and reversible, and continue until the energy reaches the dead state. Pressure drop and heat transfer holding a degree of irreversibility in every heat exchanger. Since the flowing of fluids in the heat exchangers are in touch with solid surfaces it causes friction and subsequently leads to irreversibility. This means the exergy loss or wasting the available energy instead of using it in a useful manner. The same story is true for the heat transfer but

Table 3 Uncertainty of results.

Parameter	Uncertainty
Temperature	
Hot water inlet temperature (°C)	±0.5
Hot water outlet temperature (°C)	±0.5
Cold water Inlet temperature (°C)	±0.5
Cold water outlet temperature (°C)	±0.5
Inlet air temperature (°C)	±0.5
Volumetric Flow Rate	
Hot water flow rate (lit/min)	±0.2
Cold water flow rate (lit/min)	±0.2
Air flow rate (lit/min)	±0.15
Design Parameters	
Heat transfer coefficient	±8.86%
Pressure drop	±2%
NTU	±10.16%
Exergy loss	±11.2%
Uncertainty of the physical properties read from the thermodynamic tables	
K, ρ, C_p, …	±(0.1–0.15)%

here the finite temperature difference is the factor of exergy loss. By this definition, exergy can be calculated [31] as follows:

$$\sum E_i = \sum E_o - \sum E_{product} \tag{2}$$

At the above equation $\sum E_i$ and $\sum E_o$ presents the algebraic sum of the inlet and outlet exergy, respectively. Also, $\sum E_{product}$ indicates the sum of produced exergy in the control volume or difference of inlet and outlet exergy.

Since we cannot have a completely adiabatic system, always there is a level of heat exchange between the boundaries of the system and surroundings. Hence, the total amount of heat that was expected to be transferred to the cold water cannot occur and delivers a proportion of the heat to the ambient. As a matter of fact Q_h is not equal with Q_c due to the emerged thermal irreversibility; therefore:

$$Q_h \neq Q_c \tag{3}$$

where

$$Q_h = \dot{m} c_{ph} \Delta T_h \tag{4}$$

$$Q_c = \dot{m} c_{pc} \Delta T_c \tag{5}$$

Since two working fluids (hot and cold flow) exchanging heat with each other there are two corresponding exergy destruction. So, in a steady state condition the overall exergy destruction is as follows:

$$E = E_c + E_h \tag{6}$$

That E_c refers to cold stream exergy destruction rate and E_h denotes hot stream exergy destruction rate. Each of these parameters can be obtained by:

$$E_h = T_e \dot{m}_h (s_{ho} - s_{hi}) \tag{7}$$

$$E_c = T_e \dot{m}_c (s_{co} - s_{ci}) \tag{8}$$

where T_e is the ambient temperature, also, $\dot{m}_c$ and $\dot{m}_h$ are the mass flow rate of cold and hot streams, respectively. Also, the s_{co} and s_{ci} are the specific entropy of cold flow at the outlet and inlet, respectively. Corresponding parameters of hot flow specific entropy at inlet and outlet are s_{hi} and s_{ho}.

It should be mentioned that in this study only the thermal irreversibilities are considered and the frictional irreversibilities are not included. Therefore, the entropy changes could be calculated as following:

$$s_o - s_i = c_p \ln\left(\frac{T_o}{T_i}\right) \tag{9}$$

In order to obtain the total exergy loss, Eqs. (7) and (8) should be replaced in Eq. (6) which would lead in Eq. (10):

$$E = T_e\left(\dot{m}_h c_{ph} ln\left(\frac{T_{ho}}{T_{hi}}\right) + \dot{m}_c c_{pc} ln\left(\frac{T_{co}}{T_{ci}}\right)\right) \tag{10}$$

Also, the non-dimensional exergy can be obtained as follows:

$$e = \frac{E}{T_e C_{min}} \tag{11}$$

At which the C_{min} is defined as following.

$$C_{min} = \min(\dot{m}_c c_{pc}, \dot{m}_h c_{ph}) \tag{12}$$

3.2. Calculation of number of thermal units and effectiveness

The Number of Thermal Units could be calculated as follows:

$$U_{in} = \frac{Q_{ave}}{A_{in} \Delta T_{LMTD}} \tag{13}$$

Q_{ave} can be calculated by:

$$Q_{ave} = \frac{Q_c + Q_h}{2} \tag{14}$$

where

$$Q_h = \dot{m} c_{ph} \Delta T_h \tag{15}$$

$$Q_c = \dot{m} c_{pc} \Delta T_c \tag{16}$$

Also, ΔT_{LMTD} can be calculated as follows

$$\Delta T_{LMTD} = (\Delta T_o - \Delta T_i)/\ln(\Delta T_o/\Delta T_i) \tag{17}$$

For co-current and counter flow there are different values of ΔT_{LMTD} which can be calculated as follows:

For co-current flow:

$$\Delta T_i = T_{hi} - T_{ci} \tag{18}$$

$$\Delta T_o = T_{ho} - T_{co} \tag{19}$$

For counter flow:

$$\Delta T_i = T_{hi} - T_{co} \tag{20}$$

$$\Delta T_o = T_{ho} - T_{ci} \tag{21}$$

For a double-tube heat exchanger NTU can be obtained as follows [17,18]:

$$NTU = \frac{AU}{C_{min}} \tag{22}$$

Also, effectiveness can be calculated as follows [17,18]:

$$\varepsilon = \frac{\text{Actual heat transfer}}{\text{Maximum possible heat trensfer}} \tag{23}$$

At the above equation, the Actual heat transfer could be assumed as Q_{ave}, and the maximum heat transfer could be calculated as following:

$$Q_{max} = \left(\dot{m}C_p\right)_{min}(T_{hi} - T_{ci}) \quad (24)$$

3.3. Calculation of Witte-Shamsundar efficiency

The Witte-Shamsundar efficiency (η_{w-s}) [32,33] is an effective parameter which is a good criterion for the simultaneous consideration of energy and exergy concepts for the evaluation systems. Actually this parameter considers both the quality and quantity of the heat transfer process and is very useful for the thermal engineers and experts. The Witte-Shamsundar efficiency was calculated as following.

$$\eta_{W-S} = 1 - \frac{T_0 \dot{S}_{gen}}{Q_{ave}} \quad (25)$$

In which the T_0 and Q_{ave} denote the surrounding temperature and the heat transferred in the system, respectively.

4. Results and discussion

To find the effect of made modifications on the thermal performance of the system, the results were evaluated in terms of thermal indicative concepts including Pressure drop, NTU, Effectiveness, Overall heat transfer coefficient and dimensionless thermal exergy destruction. In the present study, the cold water (annular section) flow rate was kept constant at 2 lit/min while through the inner tube the hot water flow rates varied from 3 to 6 lit/min and airflow rates varied from 1 to 5 lit/min. The VF (volume fraction) through the inner tube was between 0.14 and 0.625 which was calculated as following:

$$VF = \frac{\text{Volumetric flow rate of air}}{\text{Volumetric flow rate of water} + \text{Volumetric flow rate of air}} \quad (26)$$

4.1. Pressure drop

Fig. 2 presents the variation of the two-phase pressure drop in terms of VF (volume fraction). As presented, the increment of VF and hot water flow rate increase the two-phase pressure drop. Fig. 3 depicts the ratio of two-phase pressure drop to single phase pressure drop in terms of VF. According to results, the curves associated with this ratio finds a strict ascending form by increment of VF. Moreover, as the hot water flow rate decreases the ratio of two-phase pressure drop to single-phase pressure drop raises. This is mostly because of the fact that at lower water flow rates, adding air phase imposes more impact on pressure drop than in higher water flow rate. Indeed, at high flow rates single water-phase produces large amount of pressure drop so that induced pressure drop by air flow is low compared to that of occurred in low water flow rates. By this definition, the maximum ratio of two-phase pressure drop to single-phase pressure drop was 4.43 and was occurred at VF = 0.625.

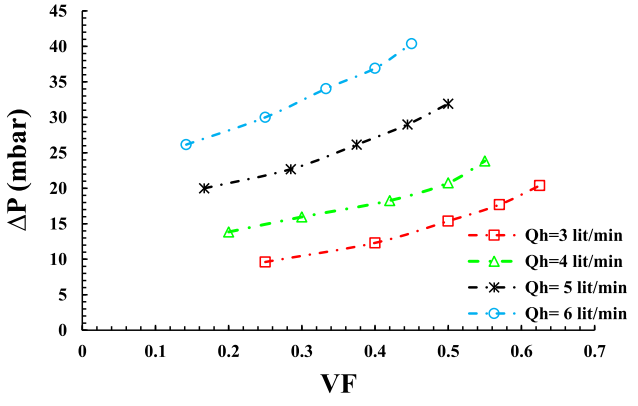

Fig. 2 Variation of ΔP_{tp} in terms of VF.

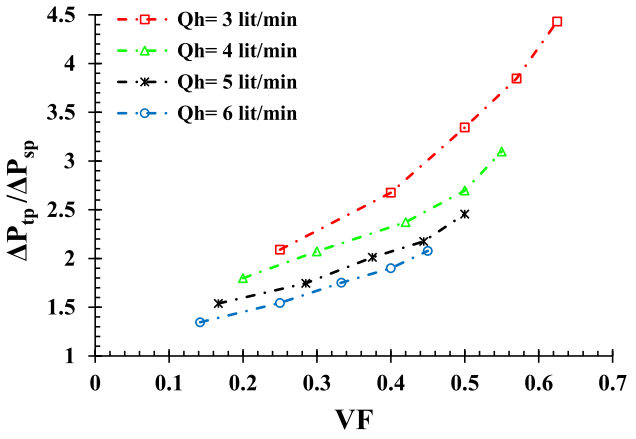

Fig. 3 Variation of $\Delta P_{tp}/\Delta P_{sp}$ in terms of VF.

4.2. Overall heat transfer coefficient analysis

Fig. 4 shows the changes in the ratio of two-phase overall heat transfer coefficient to that of single-phase in terms of VF for different hot water flow rates for both counter and parallel flows. Results demonstrate that in counter flow (Fig. 4(A)) by the increment of VF and decrement of hot water flow rate the overall heat transfer coefficient of two-phase flow be greater than that of single-phase flow. Therefore, when the VF is 0.142 and the hot water flow rate is 6 lit/min this augmentation is the least with around 8% enhancement. Conversely, the maximum improvement in the overall heat transfer coefficient is 33% and was occurred at VF and hot water flow rates are 0.625 and 3 lit/min, respectively.

As shown in Fig. 4(B), the general trend of curves indicates a slight enhancement in the overall heat transfer coefficient of two-phase flow over single phase flow. Similar to counter flow minimum enhancement in heat transfer occurs at the lowest VF and the highest hot water flow rate. This is exactly inverse when maximum heat transfer is intended. The minimum and maximum enhancements in the parallel flow were 5% and 19%, respectively.

From the literature [9,30,31,34], it is believed that two main mechanisms are engaged in the improvement of the heat transfer coefficient by air/water two-phase flow. **First**: the increment of local Reynolds number. Indeed, when two incompressible liquids flow simultaneously in a tube, the amount of cross-section for each stream decreases. As a result, and based on the continuity equation, the velocity of each stream increases. The increment of the Reynolds number causes to increment of

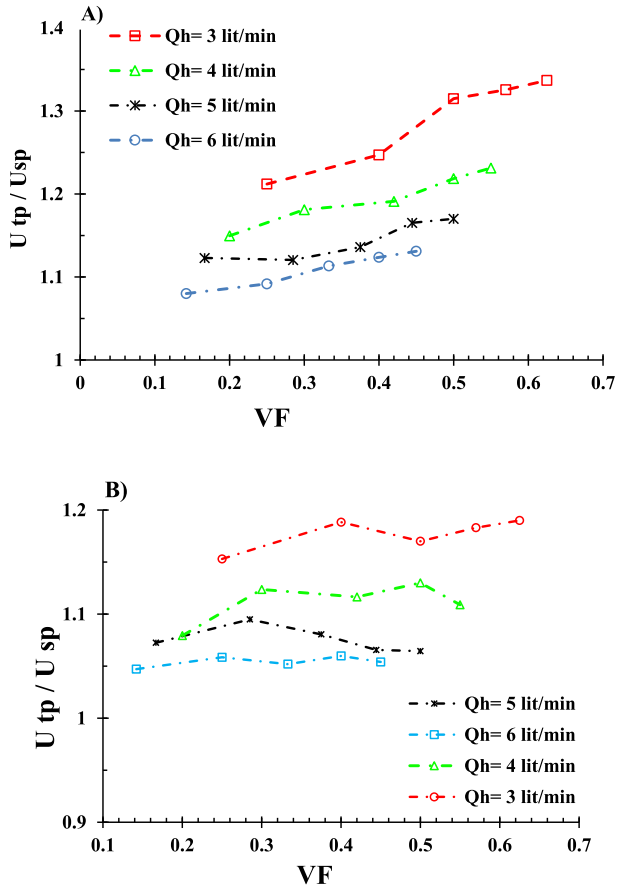

Fig. 4 Variation of U_{tp}/U_{sp} in terms of VF for: (A) Counter flow and (B) Parallel flow.

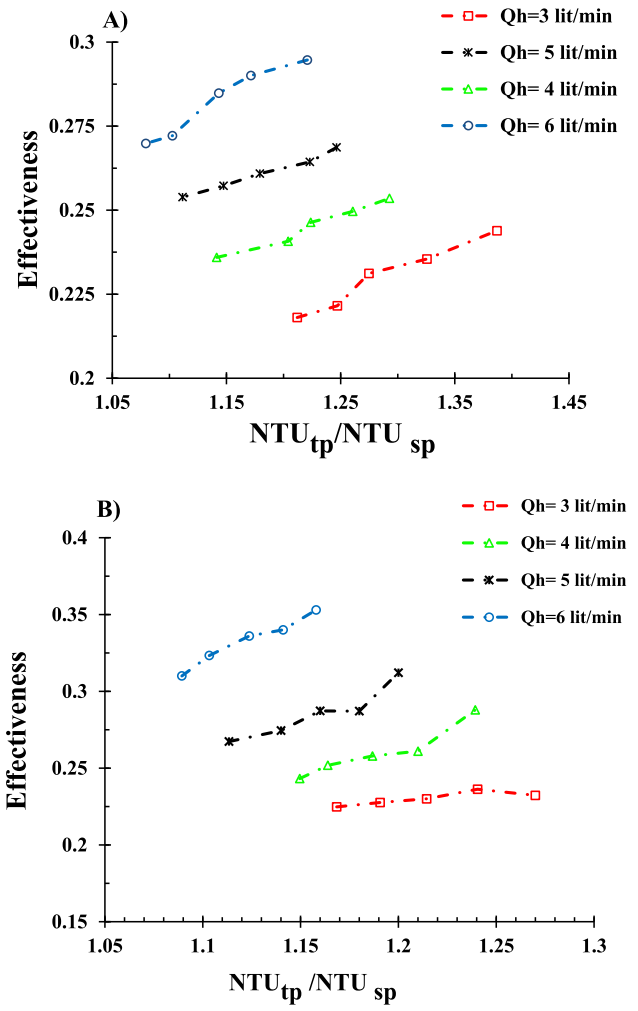

Fig. 5 Variation of effectiveness in terms of NTU_{tp}/NTU_{sp} for: (A) Counter flow and (B) Parallel flow.

the turbulence intensity of the working fluid and as a result more mixing phenomena happens in the boundary layer. Consequently, the heat transfer coefficient increases. **Second**: the contact between the air slugs and water elements. The contact between the water elements and the air slugs cause the water elements to change their moving direction. This results in appearance of fluctuations at the velocity vector of the liquid flow and as a result the turbulence intensity of the two-phase flow augments. The augmentation of the turbulence intensity is an agent of increment of mixing phenomenon in the boundary layer which prevents the boundary layer from being developed and resultantly enhances the overall heat transfer coefficient.

4.3. Number of thermal units-effectiveness analysis

Fig. 5(A) and (B) presents the the relationship between effectiveness and the ratio of two-phase NTU to single-phase NTU for both counter and parallel flow, respectively. As presented in Fig. 5(A) and (B), the overall trend of effectiveness in terms of NTU_{tp}/NTU_{sp} for each flow rate of hot water is strictly ascending. By comparing two flow arrangements, it could be found that counter flow has higher effectiveness values at all cases. In Fig. 5(A) the lowest and the highest effectiveness are related to cases in which the hot water flow rates are 3 lit/min and 6 lit/min, respectively. Similarly, these results are true for parallel flow (Fig. 5(B)) which presents the variation of aforementioned parameters for the parallel flow. In counter flow maximum effectiveness was 0.35 in whichNTU_{tp}/NTU_{sp} = 1.157 while in parallel flow maximum effectiveness was about 0.29 at which the value of NTU_{tp}/NTU_{sp} was equal to 1.22.

Fig. 6(A) and (B) shows the variation of effectiveness and NTU_{tp}/NTU_{sp}in terms of VF for both counter and parallel flow. By the increment of VF increases both effectiveness and NTU_{tp}/NTU_{sp} increase at counter flow configuration (Fig. 6(A)). Whereas, in the parallel flow (Fig. 6(B)) both effectiveness and NTU_{tp}/NTU_{sp} goes up by increment of VF for all hot water flow rates except when hot water flow rates are 6 lit/min and 5 lit/min. Indeed, as the water flow rate increases, the slugs get smaller. Consequently, a less powerful smash occurs between the air bubbles and water elements. Consequently, minor increment in the turbulence intensity of flow happens. Consequently, less heat transfer increment occurs.

4.4. Exergy analysis

The exergy is defined as the maximum reachable work of a system when it achieves to the thermally equilibrium condition with its surrounding. There are two main reasons for the

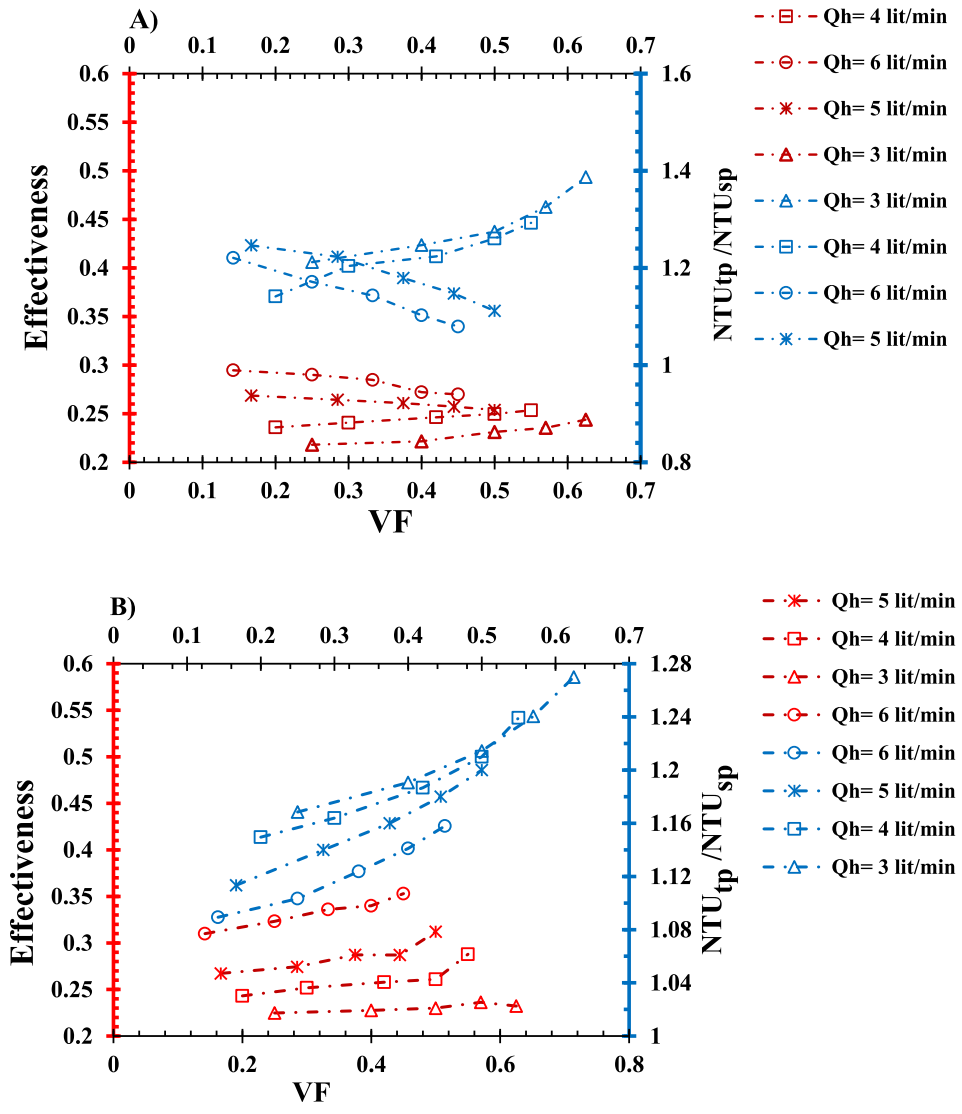

Fig. 6 Variation of effectiveness andNTU_{tp}/NTU_{sp} in terms of VF for: (A) counter flow and (B) parallel flow.

exergy destruction in the thermal systems. Firstly: heat transfer due to finite temperature difference and secondly: frictional pressure drop. In the present study as was presented in the calculation section (Section 3.1), only the exergy destruction due to heat transfer was considered. Fig. 7 (A) and (B) presents the variation of dimensionless exergy destruction of the considered heat exchanger for both counter and parallel configuration of the flow. Generally, the value of e_{tp}/e_{sp} is higher in counter flow compared to parallel flow which indicates a more efficient use of available energy. Decrement of hot water flow rate (in Fig. 7(A) and (B)) increases the e_{tp}/e_{sp}. That is because of bigger slugs of air which results in more turbulence intensity in the flow which leads to more heat transfer, which leads in more exergy loss occurs. In Fig. 7(A) as the VF goes up, the e_{tp}/e_{sp} increases too. For counter flow maximum the amount of e_{tp}/e_{sp} was about 2.071 with VF = 0.4, while in the parallel flow the highest value of e_{tp}/e_{sp} was 1.85 with VF = 0.55. It should be noted that higher exergy loss of counter flow is due to the more potential of heat transfer in the counter flow. Actually, the temperature difference of the two streams in the counter flow configuration of flow, is more than that through the parallel flow configuration. Also, this is the reason for more heat transfer coefficient and the NTU of counter flow due to the two-phase flow.

4.5. *Performance evaluation*

The effectiveness and the fraction of dimensionless form of exergy destruction, only considers the exergy and energy concepts individually. The effectiveness is related to the quantity of thermal system and the exergy concept is presents the quality of thermal systems. However, for evaluating the performance of a thermal system both of the aforementioned concepts are necessary. The Witte-Shamsundar efficiency [32,33] is a criterion that considers both the heat transfer and entropy generation in a thermal system.

Fig. 8 depicts the variation of η_{W-S} in terms of variation of VF for both counter and parallel configuration of flow in the considered heat exchanger. As is shown, the increment of VF increases the amount ofη_{W-S}. The amount of mentioned

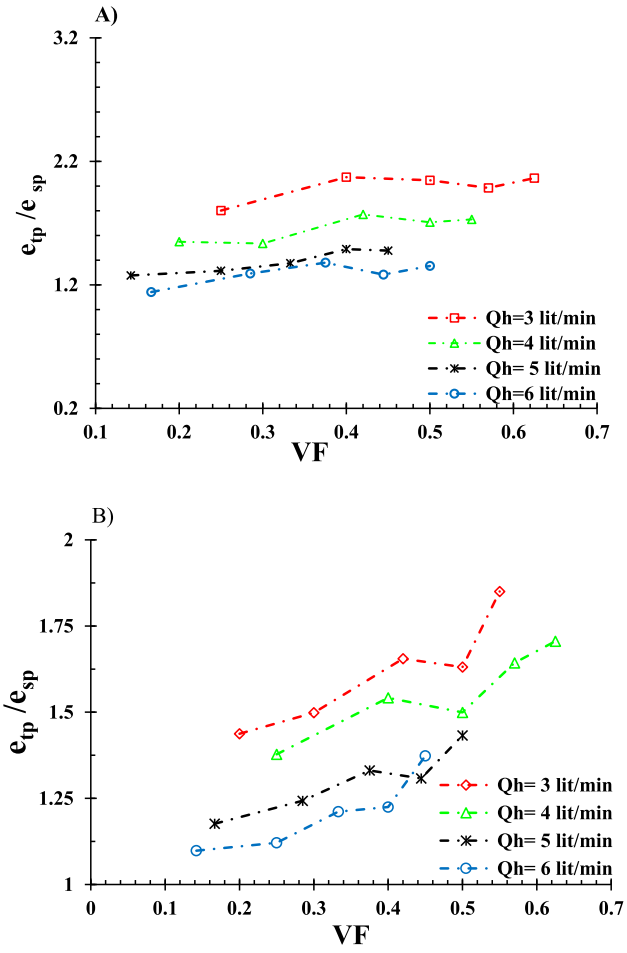

Fig. 7 Variation of e_{tp}/e_{sp} in terms of VF for: (A) counter flow and (B) parallel flow.

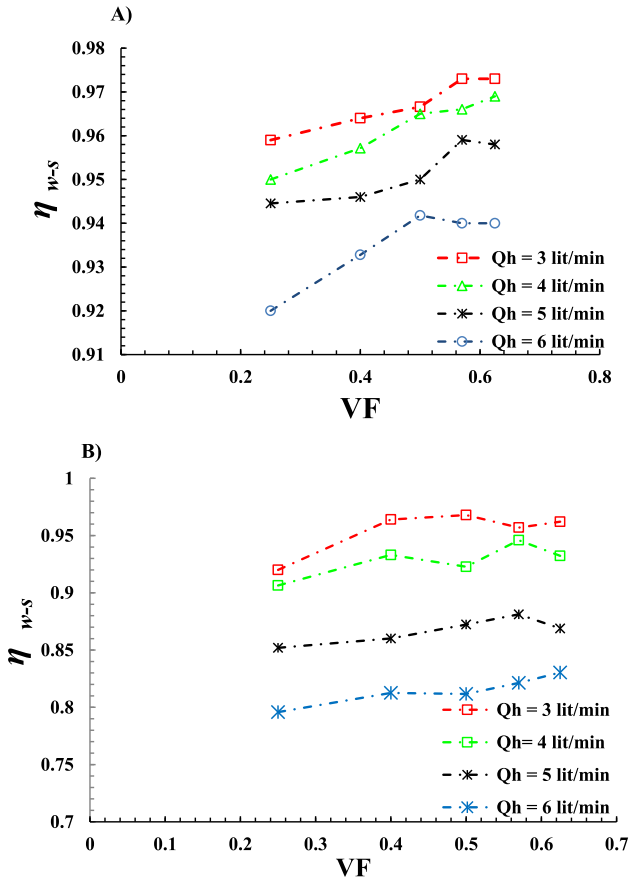

Fig. 8 Variation of η_{W-S} in terms of VF. (A) Counter follow and (B) Parallel flow.

parameter (η_{W-S}) is more, in the counter flow, denoting this point that the effect of two-phase flow in the counter flow is more than that in the parallel configuration of flow. It is shown that both in counter and parallel flow, as the hot water flow rate decreases, the amount of Witte-Shamsundar efficiency factor (η_{W-S}) increases. Generally, with the increment of VF, the values of Witte-Shamsundar efficiency factor increases too. It is because, as the water flow rate decreases the size of air slugs increases [32], so more heat transfer improvement occurs. Also, in the constant water flow rate, the increment of VF is equal with to the increment of air flow. When the amount of air compared to the water flow rate increases, the size of air slugs becomes larger. As the size of air slugs increases, the turbulence intensity of flow increases too, these phenomenon causes more mixing in the boundary layer of the of tube and as a result more heat transfer happens. Consequently, the value of the Witte-Shamsundar efficiency factor increases. The maximum amount of (η_{W-S}) was related to counter flow and to the $Q_h = 3$ lit/min and VF = 0.625, and it was equal to 0.973.

5. Conclusions

Through this paper, the influence of air/water two phase flow on thermo-exergitic performance of horizontal double tube heat exchanger was studied. The air and water streams were mixed in a T juntion outside the double tube heat exchanger and then were flowed into the inner tube of the heat exchanger. The cold water flow rate was kept constant and was equal to 2 lit/min. For the hot water flow rate, four different flow rates of 3, 4, 5 and 6 lit/min was considered. Also, for the air flow rate five different flow rates of 1, 2, 3, 4 and 5 lit/min were considered. The Volume fraction was between 0.14 and 0.62. The key results of the present study could be briefly stated as followings.

- For all hot water flow rates, with the increment of VF (volume fraction) the overall heat transfer coefficient raises. In parallel flow and counter flow, the maximum ratio of two-phase heat transfer coefficient to that of single-phase was 19% and 33%, respectively.
- In counter flow and parallel flow, the maximum effectiveness was 0.35 and 0.29, respectively.
- The increment of VF increases the ratio of two-phase NTU to single-phase NTU.
- The maximum improvement of the NTU for the counter and parallel flow was 38% and 27%, respectively.
- The increment of VF increases the exergy destruction. The maximum increment of exergy destruction through the parallel flow and counter flow, was about 85% and 106%, respectively.

- The best values of the Witte-Shamsundar efficiency (η_{W-S}) for the counter and parallel flow were 0.973 and 0.96, respectively.

CRediT authorship contribution statement

Nazaruddin Sinaga: Resources, Formal analysis, Investigation. **Saleh khorasani:** Writing - original draft, Conceptualization, Investigation. **Kottakkaran Sooppy Nisar:** Resources, Formal analysis. **Amr Kaood:** Writing - review & editing, Methodology, Formal analysis.

Declaration of Competing Interest

The authors declare that they have no known competing financial interests or personal relationships that could have appeared to influence the work reported in this paper.

References

[1] B. Zhua, B. Su, Y. Li, Input-output and structural decomposition analysis of India's carbon emissions and intensity, Appl. Energy 230 (2018) 1545–1556.

[2] L. He, Y. Chen, J. Li, A three-level framework for balancing the tradeoffs among the energy, water, and air-emission implications within the life-cycle shale gas supply chains, Resour. Conserv. Recycl. 133 (2018) 206–228.

[3] G. Wang, Y. Yao, Z. Chen, P. Hu, Thermodynamic and optical analyses of a hybrid solar CPV/T system with high solar concentrating uniformity based on spectral beam splitting technology, Energy 166 (2019) 256–266.

[4] Y. Zhang, X. Zhang, M. Li, Z. Liu, Research on heat transfer enhancement and flow characteristic of heat exchange surface in cosine style runner, Heat Mass Transf. 55 (2019) 3117–3131.

[5] M. Goodarzi, I. Tlili, H. Moria, T.A. Alkanhal, R. Ellahi, A.E. Anqi, M. Safaei, Boiling heat transfer characteristics of graphene oxide nanoplatelets nano-suspensions of water-perfluorohexane (C6F14) and water-n-pentane, Alex. Eng. J. 1 (2020), https://doi.org/10.1016/j.aej.2018.03.003.

[6] M.A.M. Ali, W.M. El-Maghlany, Y.A. Eldrainy, A. Attia, Heat transfer enhancement of double pipe heat exchanger using rotating of variable eccentricity inner pipe, Alex. Eng. J. (57) (2018) 3709–3725.

[7] A. Kumar, M. Kumar, S. Chamoli, Comparative study for thermal-hydraulic performance of circular tube with inserts, Alex. Eng. J. 55 (2016) 343–349.

[8] B. Kumar, A. Kumar Patil, S. Jain, M. Kumar, Study of entropy generation in heat exchanger tube with multiple V cuts in perforated twisted tape insert, J. Heat Transfer. 141 (8) (2019) 081801.

[9] M.F. Abd Rabbo, M.T.S. Badawy, R.Y. Sakr, A.G. Gomaa, H. R. Rashed, H.E. Fawaz, Numerical investigation of cutting edge effect on fluid flow and heat transfer for in-phase trapezoidal air channels, Alex. Eng. J. 57 (2018) 911–926.

[10] Y. Bang, S.R. Park, C.P. Cho, M. Cho, S. Park, Thermal and flow characteristics of a cylindrical superheater with circular fins, Appl. Therm. Eng. 181 (25) (2020) 115895.

[11] R. Haq, S.S. Shah, E.A. Algehyne, IskanderTlili, Heat transfer analysis of water based SWCNTs through parallel fins enclosed by square cavity, Int. Commun. Heat Mass Transfer 119 (2020) 104797.

[12] L.H.K. Goh, Y.M. Hung, G.M. Chen, C.P. Tso, Entropy generation analysis of turbulent convection in a heat exchanger with self-rotating turbulator inserts, Int. J. Therm. Sci. 160 (2021) 106652.

[13] S. Khorasani, A. Moosavi, A. Dadvand, M. Hashemian, A comprehensive second law analysis of coil side air injection in the shell and coiled tube heat exchanger: An experimental study, App. Therm. Eng. 150 (2019) 80–87.

[14] D. Panahi, Evaluation of Nusselt number and effectiveness for a vertical shell-coiled tube heat exchanger with air bubble injection into shell side, Exp. Heat Transfer (2016) 179–191, https://doi.org/10.1080/08916152.2016.1233145.

[15] S. Pourhedayat, H. Sadighi Dizaji, S. Jafarmadar, Thermal-exergetic behavior of a vertical double-tube heat exchanger with bubble injection, Exp. Heat Transfer 32 (2019) 455–468.

[16] Ha.S. Khwayyir, A.Sh Baqir, Hiba Q. Mohammed, Effect of air bubble injection on the thermal performance of a flat plate solar collector, Therm. Sci. Eng. Progr. 17 (2020).

[17] A.Sh. Baqir, H.B. Mahood, A.R. Kareem, Optimization and evaluation of NTU and effectiveness of a helical coil tube heat exchanger with air injection, Therm. Sci. Eng. Progr. 14 (2019) 100420.

[18] C. Qi, T. Luo, M. Liu, F. Fan, Y. Yan, Experimental study on the flow and heat transfer characteristics of nanofluids in double-tube heat exchangers based on thermal efficiency assessment, Energy Convers. Manage. 197 (2019) 111877.

[19] C. Qi, M. Liu, J. Tang, Influence of triangle tube structure with twisted tape on the thermo-hydraulic performance of nanofluids in heat-exchange system based on thermal and exergy efficiency, Energy Convers. Manage. 192 (2019) 243–268.

[20] M.E. Nakhchi, J.A. Esfahani, Performance intensification of turbulent flow through heat exchanger tube using double V-cut twisted tape inserts, Chem. Eng. Process. – Process Intensif. 141 (2019) 107533.

[21] A. Karimi, A.A.A.A. Al-Rashed, M. Afrand, O. Mahian, S. Wongwises, A. Shahsavar, The effects of tape insert material on the flow and heat transfer in a nanofluid-based double tube heat exchanger: Two-phase mixture model, Int. J. Mech. Sci. 156 (2019) 397–409.

[22] S. Yadav, S.K. Sahu, Heat transfer augmentation in double pipe water to air counter flow heat exchanger with helical surface disc turbulators, Chem. Eng. Process. – Process Intensif. 135 (2019) 120–132.

[23] M.M. Heyhat, A. Abdi, A. Jafarzad, Performance evaluation and exergy analysis of a double pipe heat exchanger under air bubble injection, Appl. Therm. Eng. 143 (2018) 582–593.

[24] S. Deng, C. Nie, H. Jiang, Wei-Biao Ye, Evaluation and optimization of thermal performance for a finned double tube latent heat thermal energy storage, Int. J. Heat Mass Transf. 130 (2019) 532–544.

[25] I. Bashtani, J. Abolfazli Esfahani, ε-NTU analysis of turbulent flow in a corrugated double pipe heat exchanger: A numerical investigation, Appl. Therm. Eng. 159 (2019) 113886.

[26] C. Gnanavel, R. Saravanan, M. Chandrasekaran, Heat transfer augmentation by nano-fluids and circular fin insert in double tube heat exchanger – A numerical exploration, Mater. Today: Proc. (2019), https://doi.org/10.1016/j.matpr.2019.08.236.

[27] E. Liu, L. Lv, Y. Yi, P. Xie, Research on the steady operation optimization model of natural gas pipeline considering the combined operation of air coolers and compressors, IEEE Access 7 (2019) 83251–83265, https://doi.org/10.1109/ACCESS.2019.2924515.

[28] S. Khorasani, A. Dadvand, Effect of air bubble injection on the performance of a horizontal helical shell and coiled tube heat exchanger: An experimental study, Appl. Therm. Eng. 111 (2017) 676–683.

[29] A. Moosavi, M. Abbasalizadeh, H. Sadighi Dizaji, Optimization of heat transfer and pressure drop characteristics via air bubble

injection inside a shell and coiled tube heat exchanger, Exp. Therm Fluid Sci. 78 (2016) 1–9.
[30] R.J. Moffat, Describing the uncertainties in experimental results, Exp. Therm. Fluid Sci. 1 (1988) 3–17.
[31] E. Akpinar, Y. Bicer, Investigation of heat transfer and exergy loss in concentric double pipe exchanger equipped with swirl generators, Int. J. Therm. Sci. 44 (2005) 598–607.
[32] Y. Zhang, P. Huang, Influence of mine shallow roadway on airflow temperature, Arab. J. Geosci. 13 (2020) 12, https://doi.org/10.1007/s12517-019-4934-7.
[33] L.C. Witte, N. Shamsundar, A thermodynamic efficiency concept for heat exchange devices, J. Eng. Power 105 (1983) 199–203.
[34] S. Rostami, N. Ahmadi, S. Khorasani, Experimental investigations of thermo-exergitic behavior of a four-start helically corrugated heat exchanger with air/water two-phase flow, Int. J. Therm. Sci. 145 (2019) 106030.